Evidence for Nonvectorial, Retrograde Transferrin Trafficking in the Early Endosomes of HEp2 Cells

Richik N. Ghosh and Frederick R. Maxfield

Department of Pathology, Columbia University College of Physicians and Surgeons, New York 10032

Abstract. We have previously characterized the trafficking of transferrin (Tf) through HEp2 human carcinoma cells (Ghosh, R. N., D. L. Gelman, and F. R. Maxfield. 1994. *J. Cell Sci.* 107:2177–2189). Early endosomes in these cells are comprised of both sorting endosomes and recycling compartments, which are distinct separate compartments. Endocytosed Tf initially appears in punctate sorting endosomes that also contain recently endocytosed LDL. After short loading pulses, Tf rapidly sorts from LDL with first-order kinetics ($t_{1/2}$ ~2.5 min), and it enters the recycling compartment before leaving the cell ($t_{1/2}$ ~7 min).

Here, we report a second, slower rate for Tf to leave sorting endosomes after HEp2 cells were labeled to steady state with fluorescein Tf instead of the brief pulse used previously. We determined this rate using digital image analysis to measure the Tf content of sorting endosomes that also contained LDL. With an 11-min chase, the Tf in sorting endosomes was 24% of steady-state value. This was in excess of the amount expected (5% of steady state) from the rate of Tf exit after short filling pulses. The excess could not be accounted for by reinternalization of recycled cell surface Tf, implying that either some Tf was retained in sorting endosomes, or that Tf was delivered back to the sorting endosomes from the recycling compartment. The former is unlikely since nearly all sorting endosomes contain detectable Tf after an 11-min chase, even though more than one third of the sorting endosomes were formed during that chase time. Furthermore, while observing living cells by confocal microscopy, we saw vesicle movements that appeared to be fluorescent Tf returning from recycling compartments to sorting endosomes. The slow rate of exit after steady-state labeling was similar to the Tf exit rate from the cell, suggesting an equilibration of Tf throughout the early endosomal system by this retrograde pathway. This retrograde traffic may be important for delivering molecules from the recycling compartment, which is a long-lived organelle, to sorting endosomes, which are transient.

SORTING of endocytosed macromolecules towards their final destinations occurs in the endosomes of cells (van Deurs et al., 1989; McGraw and Maxfield, 1991). Early endosomes are defined as those compartments that are accessible to molecules of the recycling pathway, such as transferrin (Tf)[1] (Schmid et al., 1988). Work on CHO and HEp2 (human epidermoid carcinoma) cells has classified early endosomes into two distinct, separate compartments: the sorting endosome and the recycling compartment (McGraw and Maxfield, 1991; Ghosh et al., 1994). Endocytosed macromolecules are delivered to the sorting endosome within 1–2 min, and it is here that ligand-receptor uncoupling and sorting for proper delivery to their next cellular destinations occur (Geuze et al., 1983; Dunn et al., 1989; Ghosh et al., 1994). Sorting endosomes contain both newly endocytosed LDL and Tf. In CHO cells, sorting endosomes are punctate peripheral compartments with short tubular extensions, and in HEp2 cells, they have a more tubulovesicular morphology (Yamashiro et al., 1984; Hopkins et al., 1990; Ghosh et al., 1994). Membrane-associated components in sorting endosomes, such as Tf bound to its receptor, other recycling receptors, and a majority of lipids, are sorted from bulk volume contents such as released ligands, and they are then delivered to the recycling compartment with first-order kinetics, perhaps by small transport vesicles ($t_{1/2}$ ~2.5 min) (Stoorvogel et al., 1987; Dunn et al., 1989; Mayor et al., 1993; Ghosh et al., 1994). The recycling compartment is a large, long-lived, condensed tubular

Address correspondence to Dr. F. R. Maxfield, Department of Pathology, Room 15-420, College of Physicians and Surgeons, Columbia University, 630 West 168th Street, New York, NY 10032. Tel.: (212) 305-4090. Fax: (212) 305-5498.

1. *Abbreviations used in this paper*: BODIPY, 4,4-difluoro-4-bora-3a, 4a-diaza-s-indacene; C_6-NBD-ceramide, *N*-(ε-7-nitrobenz-2-oxa-1,3-diazol-4-yl-aminocaproyl)-D-erythro-sphingosine; DiI, 1,1′-dioctadecyl-3,3,3′, 3′-tetramethylindocarbocyanine perchlorate; DiO, 3,3′-dioctadecyloxacarbocyanine perchlorate; F-Tf, fluorescein-conjugated transferrin; LDL-R; low density lipoprotein receptor; Tf, transferrin; Tf-R, transferrin receptor; TGN, *trans*-Golgi network.

structure near the cell's pericentriolar region in CHO cells, and it is more spread out in HEp2 cells (Yamashiro et al., 1984; Hopkins et al., 1990; Tooze and Hollinshead, 1991; Mayor et al., 1993; McGraw et al., 1993; Ghosh et al., 1994). It is a separate compartment from sorting endosomes, and it contains sorted recycling material such as Tf and recycling receptors, but not molecules destined for lysosomes.

Pulse-chase experiments with fluorescently labeled LDL have shown that lysosomally targeted ligands accumulate in the bulk volume of sorting endosomes, which eventually stop receiving freshly endocytosed material and mature into late endosomes (Dunn and Maxfield, 1992; Ghosh et al., 1994). Thus, the delivery of lysosomally directed material to late endosomes occurs by a process where the short-lived sorting endosomes mature into late endosomes. Delivery of material to late endosomes by maturation has also been shown by other methods (Murphy, 1991; Stoorvogel et al., 1991; van Deurs et al., 1993).

Early and late endosomes have different protein compositions. For example, the small GTP-binding proteins Rab4 and Rab5 appear in early but not in late endosomes, while Rab7 and Rab9 are in late but not early endosomes (Goud and McCaffrey, 1991; Pfeffer, 1992). If the sorting endosome is a short-lived organelle that matures into a late endosome, the question is raised as to how it maintains a protein composition distinct from that of late endosomes and the plasma membrane (Griffiths and Gruenberg, 1991). Current models of endocytosed material trafficking assume a vectorial Tf transport pathway, where the Tf goes from the plasma membrane to sorting endosomes, to recycling compartments, and then back to the plasma membrane (McGraw and Maxfield, 1991). However, proteins required for sorting endosome function could cycle between the long-lived recycling compartment and sorting endosomes by an intracellular route. This would require a nonvectorial trafficking pathway to exist from recycling compartments back to sorting endosomes. In this paper, we examine whether such a nonvectorial, retrograde pathway exists.

We used fluorescent Tf and LDL as probes of the recycling and lysosomally directed pathways, respectively, and quantitative confocal microscopy to simultaneously visualize their distributions in the entire HEp2 cell in three dimensions. To determine if nonvectorial trafficking in early endosomes occurs, HEp2 cells labeled to steady state with fluorescent Tf were chased for periods much longer than the Tf sorting half-time, and then the Tf content in sorting endosomes was measured. We found that after long chase times, the Tf present in sorting endosomes was more than expected, based on sorting and vectorial transport to recycling compartments. We suggest that the excess Tf arrived in sorting endosomes by a nonvectorial, retrograde pathway from recycling compartments. This is supported by fluorescence movies of live cells in which examples of nonvectorial, retrograde Tf transport were observed. The existence of nonvectorial, retrograde Tf trafficking in early endosomes resolves certain differences between arguments, favoring a maturation process for the delivery of material to late endosomes, and those favoring a stable-compartment early endosome model with delivery to late endosomes by carrier vesicles (Griffiths and Gruenberg, 1991; Murphy, 1991; Stoorvogel et al., 1991; Dunn and Maxfield, 1992; Ghosh et al., 1994).

Materials and Methods

Cell Culture

HEp2 cells were grown in bicarbonate buffered DME (Gibco Laboratories, Grand Island, NY) supplemented with 5% FBS (Gibco), 100 U/ml penicillin, and 100 μg/ml streptomycin (Gibco) at 37°C in a 5% CO_2 humidified air atmosphere. 48–72 h before an experiment, cells were plated either in six-well plastic dishes for ^{125}I-transferrin experiments, or for optical microscope experiments, in 35-mm diameter plastic tissue culture dishes whose bottoms had been replaced with polylysine-coated No. 1 glass coverslips (Salzman and Maxfield, 1988). 24 h before experiments, the medium was replaced with a similar medium but now containing 5% lipoprotein deficient serum and 4 μM deferoxamine mesylate (Sigma Chemical Co., St. Louis, MO) to stimulate increased expressions of the cells' LDL and Tf receptors (Mattia et al., 1984; Goldstein et al., 1983).

Fluorescent Labels

Fluorescein-labeled transferrin (F-Tf) was made as previously described (Yamashiro et al., 1984). 4,4-difluoro-4-bora-3a,4a-diaza-s-indacene (BODIPY)-labeled diferric-transferrin (BODIPY-Tf) was obtained from Molecular Probes, Inc. (Eugene, OR). 1,1′-dioctadecyl-3,3,3′,3′-tetramethylindocarbocyanine labeled LDL (dil-LDL) was prepared by the protocol of Pitas et al. (1981). Cy3™ was obtained from Biological Detection Systems (Pittsburgh, PA) and conjugated to transferrin as previously described (Mayor et al., 1993). *N*-(ε-7-nitrobenz-22-oxa-1,3-diazol-4-yl-aminocaproyl)-D-*erythro*-sphingosine (C_6-NBD-ceramide) was obtained from Molecular Probes.

Fluorescent Labeling of Cells

All labeling was done in air on a 37°C warm tray. Before any fluorescent labeling, the culture medium of each coverslip bottom dish was removed, and the cells were rinsed once and then incubated for 5 min with dye-free labeling medium (F-12 medium without bicarbonate, buffered with 20 mM Hepes to pH 7.4, and containing 100 U/ml penicillin, 100 μg/ml streptomycin, and 2 mg/ml ovalbumin [Sigma]). To study LDL and Tf sorting, the cells were then incubated for 2 min with 20 μg/ml F-Tf and 20 μg/ml dil-LDL in labeling medium for 2 min. To remove cell surface Tf, cells were incubated for 2 min at 37°C in a pH 4.6 citrate buffer (containing 25.5 mM citric acid, 24.5 mM sodium citrate, 280 mM sucrose, and 0.01 mM deferoxamine mesylate), followed by two rinses in a pH 7.4 chase medium (McCoy's 5A medium without bicarbonate, buffered with 20 mM Hepes to pH 7.4, and containing 100 U/ml penicillin, 100 μg/ml streptomycin, 50 μM deferoxamine mesylate, and 100 μg/ml of unlabeled transferrin). Deferoxamine mesylate was used to chelate the iron. This impermeant mild acid wash/neutral rinse procedure is a modification of the protocol of Salzman and Maxfield (1988), and it removed ~95% of the cell surface transferrin. The lack of effects of mild acid washing on cell viability and endocytic kinetics have been validated in earlier publications (Ghosh et al., 1994; Presley et al., 1993; McGraw and Maxfield, 1990; Dunn et al., 1989; Salzman and Maxfield, 1988; Thomas et al., 1979). The procedure did not affect the endocytic machinery of HEp2 cells, since the cells remained viable after the acid wash and rinses, and they could still undergo endocytosis at similar rates to cells that were not mild acid washed. In addition, the rates for Tf to leave the sorting endosome and the whole cell were similar in cells that had or had not been mild acid washed (Ghosh et al., 1994). Furthermore, Thomas et al. (1979) have shown that the cytoplasmic pH of cells remains constant for several minutes after the extracellular medium has been exchanged for an acidic one. The cells were then chased for different lengths of time in the chase medium before being fixed and prepared for microscopy. Unless otherwise noted, fixation for all experiments was in 2.5% paraformaldehyde freshly diluted in medium 1 (150 mM NaCl, 20 mM Hepes, pH 7.4, 1 mM $CaCl_2$, 5 mM KCl, and 1 mM $MgCl_2$) for 2 min. After four rinses in medium 1, SlowFade reagent (1,4-diazabicyclo-2,2,2-octane (DABCO) in glycerol/phosphate-buffered saline (Molecular Probes)) was applied. This was removed and fresh SlowFade reagent was reapplied. The SlowFade reagent reduced photobleaching of the F-Tf and did not affect dil-LDL staining.

Steady-state transferrin labeling of cells was done by first incubating the cells with 5 μg/ml F-Tf in labeling medium for 1 h. This was followed by a 4-min pulse of 5 μg/ml F-Tf and 20 μg/ml dil-LDL in labeling medium, and then fixation and SlowFade application. To test for nonvectorial, retro-

grade transferrin transport, cells were incubated for 1 h with 5 μg/ml F-Tf in labeling medium followed by the mild acid/neutral wash procedure to remove surface-bound transferrin. The cells were then chased in chase medium for 7 min followed by a 4-min pulse of 20 μg/ml diI-LDL in chase medium, and then fixed. For confocal movies, the cells were either incubated with 20 μg/ml diI-LDL and BODIPY-Tf in labeling medium, or with 20 μg/ml BODIPY-Tf in labeling medium followed by mild acid/neutral washing and then incubated with 20 μg/ml diI-LDL in chase medium, before the recording of living cells was started.

To check if Tf was in the *trans*-Golgi network (TGN), cells were incubated with 5 μg/ml Cy3™-Tf in labeling medium for 1 h, fixed for either 2 or 30 min as described above, and then labeled with 5 μM C_6-NBD-ceramide in medium 1 for 30 min at room temperature. The cells were then back-exchanged in 2.5% fatty acid free BSA (Sigma) in medium 1 (3 × 20-min changes) to remove surface C_6-NBD-ceramide before viewing (Pagano et al., 1989).

Confocal Microscopy

Fluorescence images of cells were obtained with a laser scanning confocal microscope (MRC 600; Bio-Rad Microscience, Cambridge, MA) on an inverted microscope (Axiovert; Zeiss, Oberkochen, Germany) using a 63× (NA 1.4) Zeiss Plan-Apo infinity corrected objective. The illumination sources were the 488- and 514-nm lines from a 25-mW argon laser. F-Tf was visualized with a 488-nm bandpass excitation filter, a 510-nm dichroic mirror and a 515-nm long pass emission filter. DiI-LDL was visualized with a 514-nm bandpass excitation filter, a 540-nm dichroic mirror, and a 550-nm long pass emission filter. The confocal microscope had two photomultiplier tubes enabling detection of two fluorophores simultaneously. To simultaneously visualize either F-Tf or BODIPY-Tf with diI-LDL, a 514-nm excitation filter was used. Fluorescence emissions were selected with a 527-nm dichroic mirror, and they were divided between the two photomultiplier tubes by a 565-nm dichroic mirror and a 600-nm long pass emission filter for diI-LDL, and a 525–555-nm band pass filter for fluorescein and BODIPY.

The confocal microscope was calibrated using 300-nm fluorescent beads to determine the dependence of the image slice vertical thickness on the aperture size (Wells et al., 1990). Each field of cells was sectioned three dimensionally by recording images from a series of focal planes. Moving from one focal plane to the next was achieved by a stepper motor attached to the fine focus control of the microscope, and the step sizes (range = 0.5–1.25 μm) were chosen with regard to the aperture size being used so that there would be some overlap between adjacent vertical sections. Enough vertical sections were taken so that the tops and bottoms of all the cells in each field would be recorded. A 10% neutral density filter in the excitation path was used to reduce photobleaching. Each image collected was the average of four scans at the confocal microscope's normal scan rate. Photobleaching was not a problem since diI-LDL's and BODIPY-Tf's photobleaching was negligible under these conditions, and the SlowFade reagent prevented F-Tf photobleaching. During each imaging session, calibration images were taken of: (*a*) a microscope slide containing medium 1 to measure background levels; (*b*) a slide containing diI dissolved in DMSO; and (*c*) (if needed) a slide containing F-Tf.

For the confocal movies of live cells, the microscope stage was kept at 37°C with a hot air blower. A small area (96 × 128 pixels) was imaged at faster scan speeds to improve the time resolution. Acquiring, averaging four times, and storing one slice took 1.5 s. For thick cells, several sections were taken to encompass the whole cell thickness.

Image Processing and Quantification

Image processing and quantification were done by an image processor (Gould-Vicom IP900; VICOM Visual Computing, Fremont, CA) run by a microVAX-II minicomputer (Digital Equipment Corporation, Maynard, MA), and has been described in detail elsewhere (Dunn et al., 1989; Maxfield and Dunn, 1990; Ghosh et al., 1994). We find that with the filter sets we used, diI leaked into the green detector and fluorescein leaked into the diI detector, but BODIPY did not. Thus, for dual-labeled samples, before a projection was made of the three-dimensional stack of images, each image in a stack was corrected for leakage of emission light from one fluorophore through the barrier filters into the other fluorophore's detector. This was done by measuring the fraction of leakage of one fluorophore into the other fluorophore's detector, using the calibration images of diI and F-Tf, and then subtracting that fraction of the original image from the image receiving the leaked light. To ensure this excitation light leakage correction procedure worked every time, we also labeled control dishes of cells singly with one fluorophore and recorded their images in the dual imaging mode, and then tested this correction procedure on them.

^{125}I-Transferrin Experiments

^{125}I-Transferrin (^{125}I-Tf) was prepared as previously described (Yamashiro et al., 1984). The labeling medium was 3 μg/ml ^{125}I-Tf in McCoy's 5A medium supplemented with 2 mg/ml ovalbumin, and experiments were done on monolayers of cells grown in six-well plates. ^{125}I-Tf binding specificity was checked by control experiments where the labeling medium had 200 times excess unlabeled Tf (McGraw and Maxfield, 1990). The Tf exit rate, steady-state, surface-internal Tf ratio and Tf internalization rate in HEp2 cells have all been previously measured (Ghosh et al., 1994).

The amount of cell surface Tf available for reinternalization following a pH 4.6 mild acid/neutral wash was determined by incubating cells for 2 h at 37°C with 3 μg/ml ^{125}I-Tf in labeling medium. A pH 4.6 mild acid/neutral wash was then used to remove the cell surface Tf, followed by chases for different times (0, 5, 10, and 15 min). The cells were rinsed once more with chase medium, put on ice, and incubated with ice-cold medium 1 for 5 min. The cells were then rinsed once more with ice-cold medium 1 and incubated with a harsh acid wash (0.2 N acetic acid, 0.2 N NaCl, pH ~2) for 5 min (McGraw and Maxfield, 1990). The cells were rinsed twice more with cold medium 1. The medium 1 rinses and the harsh acid wash were pooled, and their radioactivity was counted in a gamma counter, to determine the ^{125}I-Tf remaining on the surface after the mild acid/neutral wash procedure. The cells were then solubilized in 0.1 N NaOH, and their radioactivity was counted to determine how much ^{125}I-Tf was left inside the cell.

Tf Expected in Sorting Endosomes in a Vectorial Trafficking Scheme

An endocytic vectorial trafficking scheme is outlined in the following diagrams, where Tf goes from the plasma membrane (PM) to the sorting endosome (SE), to the recycling compartment (RC), and then back to the plasma membrane.

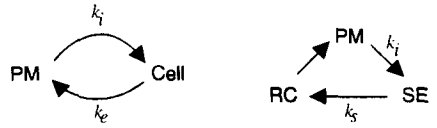

The Tf internalization rate constant is k_i, the sorting rate constant is k_s, and the rate constant for Tf to exit the cell is k_e. The rate of Tf accumulation in sorting endosomes in a vectorial pathway with first-order kinetics is

$$\frac{dT_s}{dt} = k_i T_P - k_s T_s, \tag{1}$$

where T_s is the Tf in sorting endosomes, and T_p is the Tf on the plasma membrane. This was solved for the following two situations with appropriate initial conditions: (*a*) continuous Tf accumulation for 60 min (steady-state); and (*b*) continuous Tf accumulation for 60 min followed by an acid wash removal of surface Tf and an 11-min chase.

(*a*) In the case of saturable continuous incubation, T_p is a constant, so the Tf in sorting endosomes from a vectorial trafficking pathway was solved to be

$$T_s(t) = \frac{k_e}{k_s} R_c[1 - e^{-k_s t}], \tag{2}$$

where R_c is the Tf receptors in the cell (constant), and the internalization rate is obtained from the steady-state surface/internal ratio

$$k_i = k_e \frac{T_C}{T_P} \tag{3}$$

where T_c is the Tf inside the cell (and equals R_c at steady state in the presence of a saturating concentration of Tf). Thus, the steady-state Tf in sorting endosomes (from the asymptote in Eq. 2) is

$$T_S = \frac{k_e}{k_s} R_C. \tag{4}$$

(*b*) For the case after steady-state Tf labeling where the cell surface Tf

was removed and then the cells were chased, the fraction of cell surface Tf remaining after the acid wash (λ) was experimentally determined to be 5% of the remaining total cellular Tf (see Results and Fig. 5). Thus,

$$T_P(t) = \lambda T_{tot}(t) = \lambda T_{tot}(0)e^{-k_e t}, \quad (5)$$

where $T_{tot}(t)$ is the labeled cell-associated Tf at time t. Immediately after the acid wash ($t = 0$), the cell surface Tf amount is small (~2% of total Tf) and can be rewritten as

$$T_P(0) = \lambda T_{tot}(0) \sim \lambda R_C, \quad (6)$$

where the total cell Tf is approximated by the intracellular Tf, and assuming that all of the Tf receptors were occupied at steady state by the Tf receptors inside the cell. Thus, $T_{tot}(0)$ can be rewritten as

$$T_{tot}(0) = T_C(0) + T_P(0) = R_C + \lambda R_C = (1 + \lambda)R_C \quad (7)$$

Substituting Eq. 7 into Eq. 5 and then into Eq. 1, and using Eq. 4 for the Tf in sorting endosomes at $t = 0$, we determined T_s to be:

$$T_s(t) = R_C \frac{k_e}{k_s} (\theta e^{-k_e t} + (1 - \theta)e^{-k_s t}), \quad (8)$$

where

$$\theta = \frac{\lambda(1 + \lambda)k_s k_i}{(k_s - k_e)k_e}. \quad (9)$$

Dividing the solutions of these two cases (Eq. 8 by Eq. 4) gives Γ, the ratio of Tf in sorting endosomes after steady-state labeling, acid wash and chase to that of Tf in steady-state sorting endosomes. We find that

$$\Gamma(t) = \theta e^{-k_e t} + (1 - \theta)e^{-k_s t} \quad (10)$$

Using the rate constant values from Ghosh et al. (1994) (summarized in Table I), we find that Γ, after 11 min, ranges from 7 to 9%.

Results

Excess F-Tf Is Found in Sorting Endosomes after Steady-state Labeling and 11-min Chase

We had previously determined the kinetics of Tf and LDL trafficking in HEp2 cells (Ghosh et al., 1994), and a summary of rate constants is presented in Table I. In those experiments, HEp2 cells were labeled with a brief (2-min) pulse of F-Tf and dil-LDL, followed by an impermeant mild acid wash to remove the cell surface F-Tf, and then chased for various times. The amount of F-Tf remaining in dil-LDL spots was quantified by image processing and was found to decrease with a single exponential with a 2.5-min half-time. In separate experiments, quantitation of F-Tf accumulation in dil-LDL–labeled sorting endosomes also gave the same sorting rate (Ghosh et al., 1994). In those experiments, HEp2 cells were incubated with F-Tf for different times, and a brief pulse of dil-LDL was added at the end to identify sorting endosomes, and then the amount of F-Tf in dil-LDL labeled sorting endosomes was measured by image processing.

We wanted to see if there were trafficking pathways to and from sorting endosomes other than the delivery of newly internalized material and the exit of material to recycling compartments described by the 2.5-min half-time. Although this rapid component dominates the exit of a brief F-Tf pulse from sorting endosomes, other slower trafficking pathways might exist. To look for these, we labeled cells with F-Tf for 1 h to achieve a steady-state distribution, mild acid washed them to remove cell surface Tf, and then chased for various times. The sorting endosomes were identified by labeling with dil-LDL during the last 4 min of the chase. To determine the steady-state F-Tf content in sorting endosomes, we labeled HEp2 cells with F-Tf for 1 h, added dil-LDL for the last 4 mins, and then measured the F-Tf amount in the dil-LDL–labeled spots.

A projection of three optical slices (total thickness ~1.5 μm) taken by confocal microscopy of cells labeled to steady-state with F-Tf and chased for 11 min is shown in Fig. 1 *a* (terminal 4-min dil-LDL image) and Fig. 1 *b* (F-Tf image). There was F-Tf associated with many of the dil-LDL spots in Fig. 1, *a* and *b* (*arrows*). The F-Tf in dil-LDL spots is shown in Fig. 1 *c*, where the dil-LDL image in Fig. 1 *a* was used as a mask to select the colocalized F-Tf in Fig. 1 *b*. For comparison, a projection of three optical slices of HEp2 cells labeled to steady-state with F-Tf is shown in Fig. 2 *b*, and the corresponding sorting endosomes labeled by dil-LDL are shown in Fig. 2 *a*.

The 11-min F-Tf chase time used for Fig. 1 was more than four times the 2.5-min half-time for Tf sorting and exit from sorting endosomes, so the amount of F-Tf in sorting endosomes should have been ~5% of the amount at steady-state, assuming vectorial trafficking (Table II). We measured the mean F-Tf power (integrated intensity) in dil-LDL spots in 15 fields of cells comparable to the experimental set shown in Fig. 1, *a–c*, and compared this to the mean F-Tf power in dil-LDL spots at steady state measured in 15 fields of cells comparable to Fig. 2, *a* and *b*. We found that after an 11-min chase, the F-Tf power in dil-LDL compartments was 24 ± 7% of the steady-state value (Table II). This experiment was done three more times (on five fields of cells each time) and gave the amount of F-Tf in sorting endosomes after 11 min to be 23 ± 3, 31 ± 4, and 18 ± 4% of the steady-state amounts. Combining the results from all these fields of cells, we get the amount of F-Tf in sorting endosomes after

*Table I. Summary of Measured Transferrin and LDL Trafficking Rate Constants in HEp2 Cells**

Trafficking step	Parameter	Rate constant (±SE)	Half-time
		min^{-1}	*min*
Transferrin exit from cells‡	k_e	0.09 ± 0.01 0.105 ± 0.005 0.13 ± 0.05	~7
Transferrin sorting from dil-LDL	k_s	0.28 ± 0.04	~2.5
Transferrin internalization	k_i	0.167 ± 0.009	~4
Sorting endosome maturation	k_m	0.04 ± 0.01	~17

* Ghosh et al. (1994).
‡ The values for k_e are from three different methods of measuring transferrin exit from cells (i.e., F-Tf and ^{125}I-Tf washout and F-Tf accumulation in cells, respectively).

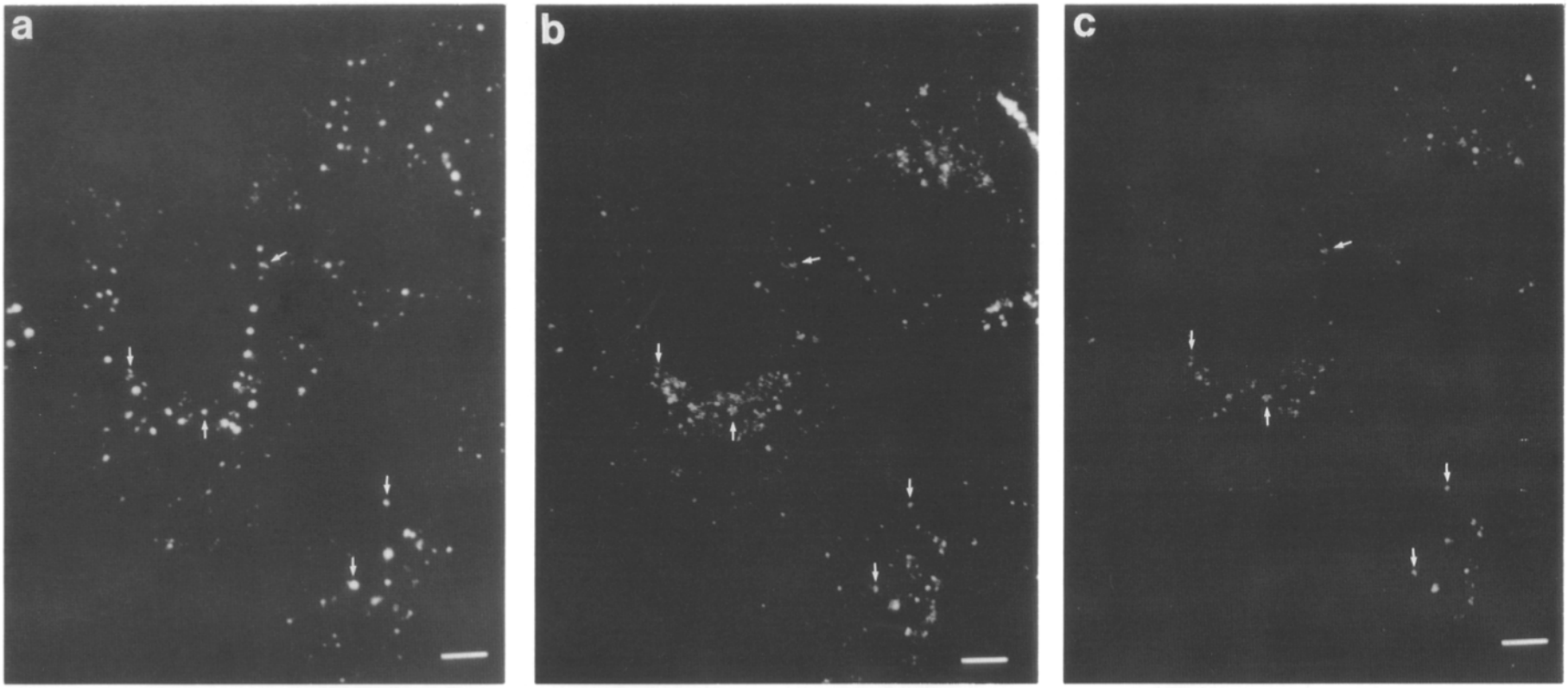

Figure 1. HEp2 cells were labeled with 5 μg/ml F-Tf for 1 h, mild acid washed, chased for 7 min, and then labeled for 4 min with 20 μg/ml diI-LDL to identify sorting endosomes. These images are a projection of three optical slices of the cell taken by confocal microscopy corresponding to a total thickness of ~1.5 μm. diI-LDL staining is in *a* and F-Tf in *b*. F-Tf was still in diI-LDL–labeled sorting endosomes (*arrows*), and this is shown in *c*, where the colocalized F-Tf regions in *b* were selected by a mask made of the diI-LDL image in *a*. Bar, 5 μm.

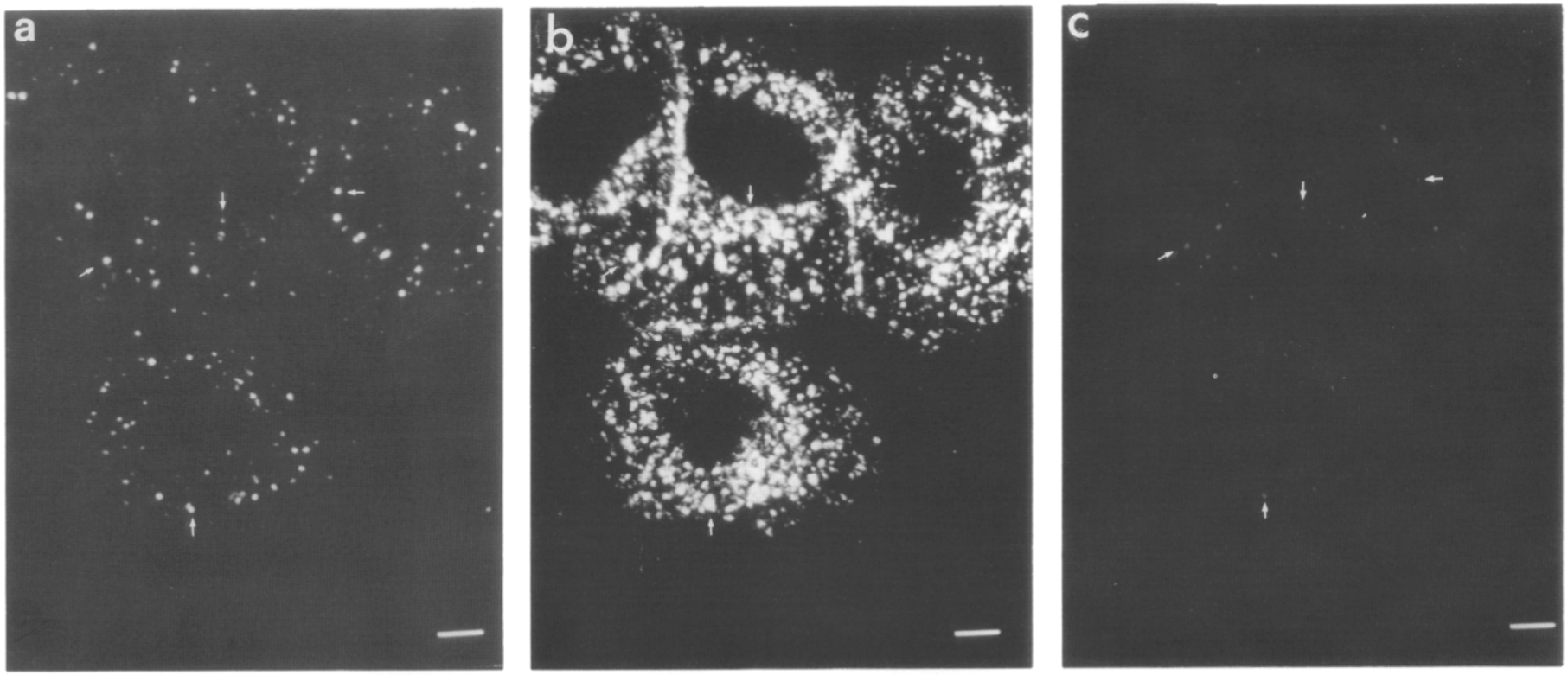

Figure 2. Steady-state labeling of HEp2 cells with F-Tf. Cells were labeled with 5 μg/ml F-Tf for 1 h, and 20 μg/ml diI-LDL was added during the last 4 min of F-Tf labeling to identify sorting endosomes. These images show a projection of three optical slices of the cell taken by confocal microscopy corresponding to a total thickness of ~1.5 μm. DiI-LDL staining is in *a* and F-Tf in *b*. To visualize the F-Tf in sorting endosomes if a vectorial trafficking scheme with Tf reinternalization existed, the F-Tf image in *b* was divided by 12 (~×8%), selected by a mask of the diI-LDL image in *a*, and shown in *c*. Arrows mark sorting endosomes and their contents in these figures. Bar, 5 μm.

Table II. Summary of Transferrin in Sorting Endosomes under Various Conditions

Condition	Transferrin (% of steady-state value)
Steady state	100
Expected after 11-min chase (vectorial trafficking; no Tf on surface)*	5
Expected after 11-min chase (vectorial trafficking; 5% of total Tf on surface)‡	8
Experimentally observed after 11 min§	24

* Calculated value for the amount of Tf remaining in sorting endosomes if Tf left sorting endosomes with first-order kinetics and if there was no reinternalization of Tf from the cell surface. This was based on the experimentally determined value for k_s (0.28 min^{-1}).
‡ Calculated value for vectorial trafficking, but also accounting for the small amount of Tf reinternalization, using equation 10 and the experimentally determined amount of Tf that returns from the cell surface bound to receptors.
§ Mean experimentally measured Tf in sorting endosomes after 11 min chase from four separate experiments (measured values were 24 ± 7%, 23 ± 3%, 31 ± 4%, and 18 ± 4%; 5–15 fields of cells per experiment).

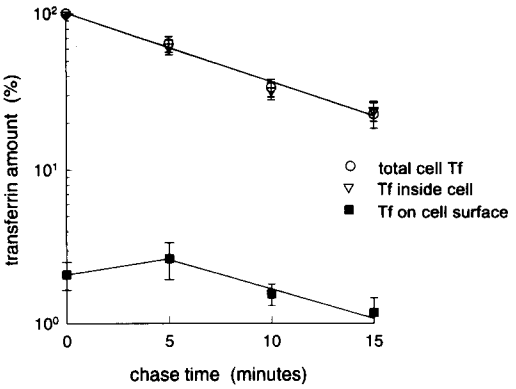

Figure 3. Determining the recycled Tf amount that remains on the HEp2 cell surface instead of dissociating from its receptor. Cells were labeled with 3 μg/ml ^{125}I-Tf for 1 h, mild acid/neutral washed to remove cell surface Tf, and then chased for various times. A 5-min harsh acid wash with rinses, which removed all the cell surface ^{125}I-Tf, was counted. The internal Tf was determined by then solubilizing the cells and counting. The total cell-associated ^{125}I-Tf at the different chase times was determined by adding the surface and internal ^{125}I-Tf counts; it is shown normalized to the 0-min value (○), and it has a single exponential decrease with approximately 7-min $t_{1/2}$, as expected (Table I). The ^{125}I-Tf inside the cell (▽) and the ^{125}I-Tf on the cell surface (■) are also plotted as a percentage of the total cell amount at 0 min, and both also decrease with time. Normalizing the ^{125}I-Tf on the surface to the total amount of ^{125}I-Tf at each time point showed that the percentage of total cell ^{125}I-Tf on the cell surface was initially at 2%, but then by 5 min, had risen to a constant 5% of the total. Data shown is an average over four experiments, and the error bars are the SEMs. ○, total cell Tf; ▽, Tf inside cell; ■, Tf on cell surface.

11 min to be 24 ± 1%. We next examined whether this excess F-Tf resulted from the reinternalization of recycled F-Tf.

Excess F-Tf in Sorting Endosomes Is Not from Reinternalization

Although most Tf is converted to apo-Tf inside the endosomes and released rapidly upon return to the surface, it seemed possible that some Tf remained receptor bound and was reinternalized. To determine if the excess F-Tf in sorting endosomes resulted from recycled diferric F-Tf that was reinternalized by the cell, we first determined how much cell surface Tf was available for reinternalization after a mild acid wash and a neutral pH chase. We incubated HEp2 cells to steady-state with ^{125}I-Tf. After mild acid washing to remove the cell surface Tf, we chased the cells for different times and measured the surface/internal ratio of ^{125}I-Tf. The total cell-associated ^{125}I-Tf (surface plus internal) decreased with a half-time of ~7 min (Fig. 3), in agreement with the previously determined exit rate constant of 0.105 ± 0.005 min^{-1} (Ghosh et al., 1994). The internal ^{125}I-Tf decreased at a similar rate, and the cell surface ^{125}I-Tf also decreased as shown in Fig. 3. Normalizing the cell surface ^{125}I-Tf to the total cell ^{125}I-Tf at each time point, we found that the percentage of total cell ^{125}I-Tf at the cell surface was initially ~2%, and then rose and remained constant at ~5%. Thus, ~5% of the total cell Tf was on the plasma membrane during a chase and could have been reinternalized into sorting endosomes.

We next determined how much F-Tf we would expect in sorting endosomes from reinternalization after labeling to steady state followed by an 11-min chase. Assuming a vectorial trafficking scheme for F-Tf through the endocytic organelles and allowing for F-Tf reinternalization during the chase, we expect the F-Tf in sorting endosomes after an 11-min chase to have been 8% of the amount at steady state (see Eq. 10 in Materials and Methods). To visualize this prediction, we multiplied the steady-state F-Tf image in Fig. 2 *b* by 0.08, used the dil-LDL image in Fig. 2 *a* as a mask to select the colocalized regions, and displayed the result in Fig. 2 *c*. This image demonstrates how much F-Tf would have been in sorting endosomes from a purely vectorial trafficking scheme with reinternalization. Very little F-Tf was associated with sorting endosomes in Fig. 2 *c*, compared with the actual F-Tf associated with sorting endosomes after an 11-min chase in Fig. 1, *b* and *c*. Thus, F-Tf reinternalization cannot account for the excess in sorting endosomes since there was more (24% of steady state; Fig. 1, *b* and *c*) than could be accounted for by reinternalization in a vectorial trafficking scheme (8% of steady state; Fig. 2 *c*) (Table II).

The prediction of 8% of steady-state F-Tf expected in sorting endosomes after an 11-min chase was determined using the values of three trafficking rate constants measured for HEp2 cells. These are (*a*) the Tf sorting rate constant k_s (0.28 ± 0.04 min^{-1}), (*b*) the Tf exit rate constant, k_e (0.105 ± 0.005 min^{-1}), and (*c*) the Tf internalization rate constant k_i (0.167 ± 0.009 min^{-1}) (Table I). Individually varying the values of these rate constants over a wide range (more than three standard deviations) still kept the expected Tf amount in sorting endosomes lower than the experimentally determined value of 24% of steady state. The range of rate constants' values we tested was much larger than the errors in experimentally determining the actual values (Ghosh et al., 1994). Thus, the prediction of nonvectorial Tf transport is robust against a wide tolerance in the values of the trafficking rate constants.

Sorting Endosomes Filled to Steady-state with F-Tf Reveal a Second, Slower Exit Rate after Long Chases

We did similar experiments to those shown in Figs. 1 and 2, but with different chase times, and we quantified the F-Tf remaining in sorting endosomes (Fig. 4). The data at various times were well fit by a single exponential decay, and the rate constant for Tf exit from sorting endosomes after labeling to steady state is 0.124 ± 0.003 min^{-1} ($t_{1/2}$ ~5.6 min). As seen in Table I, this is much slower than k_s, the rate of Tf sorting from LDL after a short pulse with Tf. The F-Tf expected in sorting endosomes from a vectorial trafficking scheme with reinternalization was also computed for different chase times using Eq. 10 and plotted in Fig. 4. The measured F-Tf in sorting endosomes was more than this vectorial trafficking prediction for all chase times. Thus, we have now identified two Tf exit rates from sorting endosomes: (*a*) a fast rate with a 2.5-min half-time, which is detected if sorting endosomes are labeled by a brief F-Tf pulse; and (*b*) a slower rate detected after the cells were labeled to steady state. This slower rate means that there is much more F-Tf in sorting endosomes after chasing than was expected from an exit rate with the 2.5-min half-time.

Excess F-Tf in sorting endosomes could occur by three mechanisms: (*a*) a fraction of the F-Tf accumulates in the sorting endosome during a long incubation and never leaves as it matures into a late endosome; (*b*) a fraction of F-Tf leaves sorting endosomes at the slower rate measured in Fig. 4; or (*c*) some of the F-Tf that leaves sorting endosomes is returned to them. We have examined these possibilities experimentally as described below.

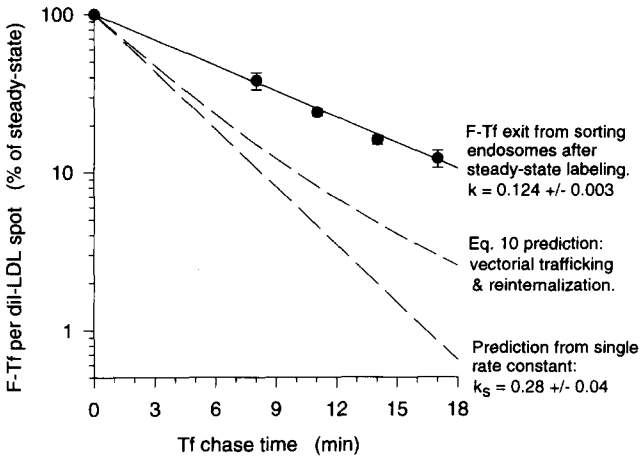

Figure 4. Exit of steady-state F-Tf from sorting endosomes. HEp2 cells were labeled with 5 μg/ml F-Tf for 1 h, mild acid washed, and then chased for various times. A terminal 4-min pulse of 20 μg/ml dil-LDL before fixation labeled the sorting endosomes. The mean amount of F-Tf in all the dil-LDL-labeled spots was measured (from 5–30 separate fields of cells recorded per time point) and plotted as a percentage of the steady-state F-Tf per dil-LDL spot (•). The F-Tf decrease in dil-LDL spots was well fit with a single exponential decay giving a rate constant of 0.124 ± 0.003 min^{-1}. Also plotted (*dashed lines*) are the amounts expected in sorting endosomes from vectorial trafficking schemes using only the forward sorting rate (0.28 ± 0.04 min^{-1}), and if the reinternalized F-Tf was accounted for (Eq. 10). Error bars are the SEMs from all the fields of cells determining each particular time point.

Excess F-Tf in Sorting Endosomes Is Not Caused by Retention or a Slowly Leaving Population

A retained population would cause the F-Tf remaining in sorting endosomes to flatten out at long chase times. However, if all the F-Tf did leave sorting endosomes, then the amount of F-Tf in the sorting endosomes would continue decreasing exponentially. The F-Tf in sorting endosomes decreased exponentially (Fig. 4), and there was no flattening above the error bars at later chase times, implying that there is no detectable retention of F-Tf in sorting endosomes. However, these data do not exclude the possibility that a fraction of the F-Tf could leave sorting endosomes with the slow rate measured in Fig. 4.

To examine this possibility, we took advantage of the observation that new sorting endosomes are being formed continuously (Dunn and Maxfield, 1992; Ghosh et al., 1994). Thus, the dil-LDL–labeled sorting endosome population at a particular chase time consists of sorting endosomes that were labeled with F-Tf during the original filling pulse, as well as those sorting endosomes formed during the chase period in the absence of F-Tf. If there was a fraction of F-Tf that left sorting endosomes with a slower rate or was retained, then at long chase times there would be some older sorting endosomes that still contained F-Tf. However, the newer sorting endosomes formed during the chase period would not have any F-Tf at all. We had previously found that 50% of the sorting endosomes become inaccessible to newly internalized material and mature in 17 min (see Table I and Ghosh et al., 1994). Thus, to maintain a constant number of sorting endosomes, ~36% of the sorting endosomes would have been formed during an 11-min chase time and should not contain any F-Tf.

Fig. 5 shows a histogram of the F-Tf powers measured in sorting endosomes after steady-state labeling and 11-min chase. The data are from single confocal slices of 15 different fields of cells from the experiment shown in Fig. 1. We found only 0.3% of all sorting endosomes contained no F-Tf, and not 36%, as expected if the source of the excess Tf was a fraction that was slowly leaving or being retained.

These results suggest that the excess F-Tf in sorting endosomes was caused by process that could deliver Tf to both old and newly formed sorting endosomes because then all the sorting endosomes after 11-min chase would be expected to contain F-Tf. Since we have ruled out reinternalization, there are two possible sources for the T-Tf delivered back to sorting endosomes: (*a*) F-Tf is transported back to sorting endosomes from recycling compartments by an intracellular route; or (*b*) small amounts of F-Tf that had been delivered to other destinations such as the TGN or lysosomes are delivered back to sorting endosomes. We examined these possibilities.

Excess F-Tf in Sorting Endosomes Implies Delivery from Recycling Compartments

Since most Tf goes from the sorting endosome to the recycling compartment before leaving the cell (Dunn et al., 1989; Mayor et al., 1993; Ghosh et al., 1994), it seems most likely that the excess F-Tf is being delivered back to sorting endosomes from the recycling compartment. However, a small amount of internalized Tf receptor has been shown to pass through the TGN (Snider and Rogers, 1985; Stoorvogel

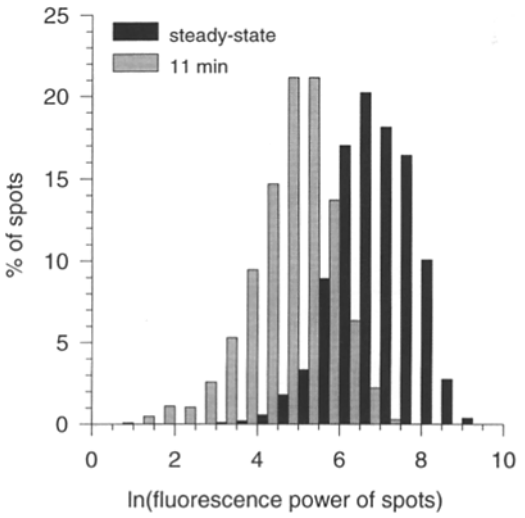

Figure 5. Histogram of the natural log of the fluorescence from F-Tf in sorting endosomes. The fluorescence power of F-Tf in each diI-LDL–labeled spot (sorting endosome) was measured from a single confocal slice from 15 different fields of cells labeled to steady-state with F-Tf, and 15 fields labeled to steady-state, then mild acid washed and chased for 11 min. These were from the same experiments used in Figs. 1 and 2. The distributions are plotted as a percentage of all the diI-LDL–labeled spots, and there were a total 1,052 and 1,436 diI-LDL spots for the steady-state and 11-min chase cases, respectively. The first column includes diI-LDL spots with no F-Tf, which is 0.3% of all diI-LDL spots for the 11-min chase case, and none for the steady-state case.

et al., 1988). Thus, we tried to determine if the source of the excess Tf in sorting endosomes could be the TGN. We first labeled HEp2 cells with Cy3™-Tf for 1 h, and then labeled the cells with C_6-NBD-ceramide, which is a probe for the TGN (Pagano et al., 1989). We found no systematic colocalization between theCy3™-Tf–labeled structures and the C_6-NBD-ceramide–labeled structures, although they were often adjacent to one another (data not shown). Thus, it does not seem likely that a significant fraction of the fluorescent Tf is in the TGN after a 1-h steady-state labeling.

Since a 1-h Tf labeling period might allow a slow-filling minor pathway to become labeled, we also labeled cells for 20 min before mild acid washing and chasing for 11 min (with diI-LDL present for the last 4 min). If the excess Tf in the sorting endosomes came from a slowly equilibrating pool, the amount should be reduced after a shorter labeling period. We found that the amount of T-Tf in sorting endosomes after 11-min chase was the same whether the F-Tf had been incubated for 20 min or for 1 h (19 ± 5 and 20 ± 7% of the steady-state amount, respectively). This is consistent with the excess Tf coming from the major intracellular source, the recycling compartment. To find direct evidence for this, we observed live cells to find examples of retrograde transport occurring.

Confocal Movies of Live Cells Show Nonvectorial Transport of Tf

We made confocal microscope movies of live HEp2 cells labeled with diI-LDL and BODIPY-Tf to directly observe vesicle movement and fusion. Taking advantage of the confocal microscope's background rejection properties, we could observe the dynamics of both labels simultaneously inside the cells while the extracellular solution still contained fluorescent labels. Thus, the live cells could undergo endocytosis and sorting while we observed them. The microscope stage was kept at 37°C. Time resolution was improved by scanning small regions (128 × 96 pixels) and observing flatter cells (requiring fewer sections per cell). Photobleaching was minimal during the time course of the movies because diI-LDL and BODIPY-Tf are photo-stable dyes, and recordings were done for short times (few minutes) to minimize illumination.

Fig. 6 shows five sets of color images from various confocal movies. These recordings are of flat cells where almost the entire thickness of the cells was observable within the depth of field of a single focal plane (~1.5 μm). The time between frames was ~1.5 s, and the movies were 50–100 frames long. The compartments containing diI-LDL alone are red, those with BODIPY-Tf alone are green, and structures containing both fluorescent ligands appear yellow to orange. We have previously identified the fluorescent structures in HEp2 cells as (*a*) sorting endosomes containing both LDL and Tf; (*b*) late endosomes or lysosomes with only LDL; and (*c*) recycling compartments containing only Tf (Ghosh et al., 1994).

Fig. 6, *a–c* shows frames from three different movies taken under steady-state BODIPY-Tf–labeling conditions, where the cells were labeled with BODIPY-Tf and diI-LDL together for ~20 min. The numbers on the figures indicate the frame number in the sequence of each movie. In the movie strip shown in Fig. 6 *a*, we saw a vesicle labeled with BODIPY-Tf (frame 19) moving to the right and apparently fusing with an organelle containing both diI-LDL and BODIPY-Tf (frames 21 and 23; *white arrow*). The BODIPY-Tf remained with the diI-LDL spot and did not emerge from the other side (frames 24 and 27). In Fig. 6 *b*, a BODIPY-Tf–labeled vesicle (frame 21) moved to the right and apparently fused with a dual-labeled organelle (frame 25; *white arrow*). The two labels then stayed together as the whole organelle moved (frames 27, 29, and 31). In Fig. 6 *c*, the BODIPY-Tf–labeled vesicle (frame 11) moved to the left and apparently fused with a dual-labeled organelle (frames 14 and 17; *white arrow*), and then the two labels remained together (frames 20 and 21). Since these movie images are made of single slices, organelles that vary their elevation during the course of their motion will fluctuate in their fluorescence intensity (e.g., frames 20 and 21 in Fig. 6 *c*). Thus, these movies can not be used for quantitation, but they do provide a qualitative picture of what is happening in the cell.

Fig. 6, *d* and *e*, are different time segments from a movie where the cells were labeled for ~30 min with BODIPY-Tf, mild acid washed, and then chased with diI-LDL for 8 min. Since the BODIPY-Tf was pulsed and then chased only a small amount of it remains in the cell, and thus its signal-to-noise was poor. To better observe the labeled organelles, we spatially averaged both the BODIPY-Tf and diI-LDL images with a Gaussian kernel and then displayed them using a logarithmic intensity scale to emphasize the dimly labeled structures. A problem with this spatial averaging is that structural details are smeared. Nonetheless, we saw examples of BODIPY-Tf–labeled vesicles joining and fusing with diI-LDL–labeled organelles in this pulse-chase experiment. In Fig. 6 *d*, a BODIPY-Tf–labeled vesicle moved to the left and apparently fused with a diI-LDL–labeled organelle (frames

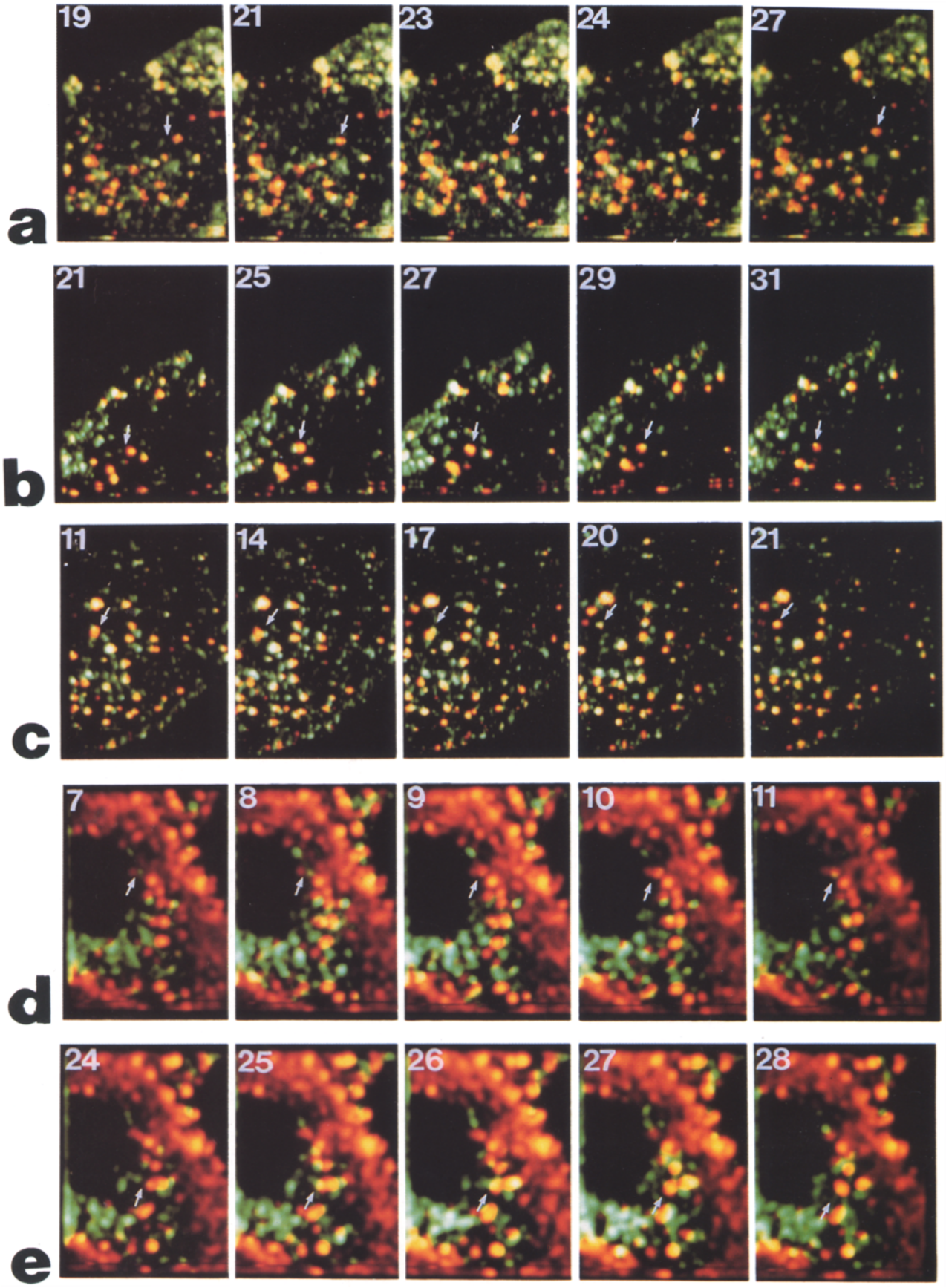

Figure 6. Image sequences from confocal movies showing nonvectorial, retrograde Tf motion. (*a–c*) The cells were incubated with 20 μg/ml diI-LDL and BODIPY-Tf for ~20 min, and were then viewed and recorded on the confocal microscope with the labels still present.

7 and 8; *white arrow*) and remained with it in subsequent frames (frames 9–11). In Fig. 6 *e*, another BODIPY-Tf–labeled vesicle in a different part of the cell (frame 24) moved to the right and apparently fused with a dil-LDL–labeled organelle (frames 25 and 26; *white arrow*), and remained with it in subsequent frames (frames 27 and 28).

Since a vesicle containing only BODIPY-Tf implied that it was a postsorting recycling compartment, its fusion with a dual-labeled (in the steady-state experiments) or dil-LDL–labeled (in the pulse-chase experiments) sorting endosome implied retrograde transport of BODIPY-Tf back to sorting endosomes. These qualitative observations of retrograde transport in live cells, while not definitive by themselves, strengthen the case for retrograde transport from recycling compartments to sorting endosomes.

Discussion

We have previously shown that Tf and LDL are initially delivered to punctate sorting endosomes in HEp2 cells (Ghosh et al., 1994). We had also shown that Tf rapidly sorts from LDL and enters tubular extensions emanating from the LDL-containing volume of the sorting endosome ($t_{1/2}$ ~2.5 min). The Tf is then delivered to a post-sorting recycling compartment and exits the cell ($t_{1/2}$ ~7 min). We have presented both morphological and kinetic evidence that recycling molecules, such as Tf, go through two distinct compartments, the sorting endosome and the recycling compartment (Ghosh et al., 1994). A summary of Tf trafficking rates is given in Table I, and we have also previously shown that Tf exit from both sorting endosomes and from inside the cell follows first-order kinetics. The sorting endosome continues to receive internalized material for a period of time ($t_{1/2}$ ~17 min) until it loses the ability to accept any more newly endocytosed LDL and matures into a late endosome.

In a simple vectorial trafficking scheme where a small percentage of the total Tf was reinternalized after recycling, we expected the Tf in sorting endosomes after steady-state labeling and 11-min chase to be ~8% of the steady-state value. Experimentally, we found that the Tf in sorting endosomes after 11 min was ~24% of the steady-state value. Several forms of evidence suggest that the excess Tf in sorting endosomes resulted from nonvectorial, retrograde transport from recycling compartments. We rule out the retrograde transport of Tf to sorting endosomes via the TGN because colocalization of the TGN with the steady-state Tf distribution in cells was not observed (data not shown). Very slowly equilibrating pools of Tf are not the source of excess Tf in sorting endosomes since short (20-min) steady-state F-Tf incubations gave the same amount of F-Tf in sorting endosomes after 11 min, as did long incubations (1 h). In addition, we rule out the excess F-Tf in sorting endosomes being caused by a permanently retained population since Tf leaves the sorting endosome after steady-state labeling with a single exponential decay, and no stably accumulated amount is seen at long chase times. We also found that essentially all the sorting endosomes after an 11-min chase contained F-Tf, indicative of F-Tf delivery to all sorting endosomes, including those formed after F-Tf was removed from the incubation medium. This is contrary to what would be expected if a slowly leaving population were the reason for the excess in sorting endosomes, because then the 36% of all sorting endosomes that would have formed during the chase would not contain F-Tf. We also find examples of retrograde Tf trafficking in live cells when viewed by confocal microscopy (Fig. 6). Fig. 7 is a schematic diagram summarizing our endocytic trafficking results in HEp2 cells.

The reason we did not detect the second, slower rate for F-Tf to leave sorting endosomes in our earlier experiments is that the occupancy of Tf receptors (Tf-R) in the recycling compartment would be low after a 2-min pulse and various chases. Thus, the amount of returning F-Tf was small compared to the amount in sorting endosomes from the initial 2-min pulse. We did not detect the small contribution of the returning F-Tf which was within the experimental limits of detection. Thus, in our earlier experiments, we measured the bulk of the F-Tf leaving with fast kinetics. However, after longer labeling periods, more F-Tf would be returned from the recycling compartment to sorting endosomes and would become detectable.

After 11 min of chase, 32% of the intracellular Tf-R are still occupied by Tf, based on measured efflux kinetics (Fig. 3) and the surface/internal ratio of Tf-R (Ghosh et al., 1994). At that time, the receptor occupancy resulting from reinternalization and forward vectorial traffic is 8%. The observation that the receptor occupancy in sorting endosomes (24%) is close to 32% implies that there is substantial retrograde traffic and that a significant fraction of the sorting endosomes' membrane comes from the recycling compartment. Further evidence for extensive equilibration between the recycling compartments and sorting endosomes is provided by the rate constant for Tf exit from sorting endosomes after labeling to steady-state (Fig. 4), which is close to the overall rate of Tf exit from the cells.

The excess Tf seen in sorting endosomes and its implication of nonvectorial, retrograde Tf trafficking could either be

(*d* and *e*) The cells were incubated with 20 μg/ml BODIPY-Tf for ~30 min, mild acid washed, and then chased with 20 μg/ml dil-LDL for 8 min. The pulse-chase sequences in *d* and *e* are from the same movie at different times showing two occurrences of retrograde Tf motion in different areas of the cell. Image frames were taken at a rate of one every 1.5 s. Five frames are shown from each movie, and the numbers indicate the frame number in the movie sequence. The cells were flat, so the entire vertical extent of the cells were visible in the 1.5 μm depth of field of the focal plane. The compartments containing dil-LDL are red, those with BODIPY-Tf are green, and structures containing both fluorescent ligands appear yellow to orange. To improve the poor signal-to-noise of the BODIPY-Tf in the pulse-chase experiment shown in *d* and *e*, the images were spatially averaged with a Gaussian kernel and then displayed with a logarithmic intensity scale to emphasize the dimly labeled compartments. The white arrows in each frame indicate the orange/red sorting endosome containing dil-LDL, to which a green BODIPY-Tf–labeled vesicle moved towards and fused. In each sequence, the green BODIPY-Tf vesicle was initially seen apart from the orange/red–labeled sorting endosome (frames 19 in *a*, 21 in *b*, 11 in *c*, 7 and 8 in *d*, and 24 in *e*). This green vesicle then moved towards and fused with the orange/red sorting endosome (frames 21 and 23 in *a*, 25 in *b*, 14 and 17 in *c*, and 25 and 26 in *e*). The fused BODIPY-Tf then remained with the sorting endosome (frames 24 and 27 in *a*, frames 27, 29, and 31 in *b*, 20 and 21 in *c*, 9–11 in *d*, and 27 and 28 in *e*). The width of each image is 27 μm.

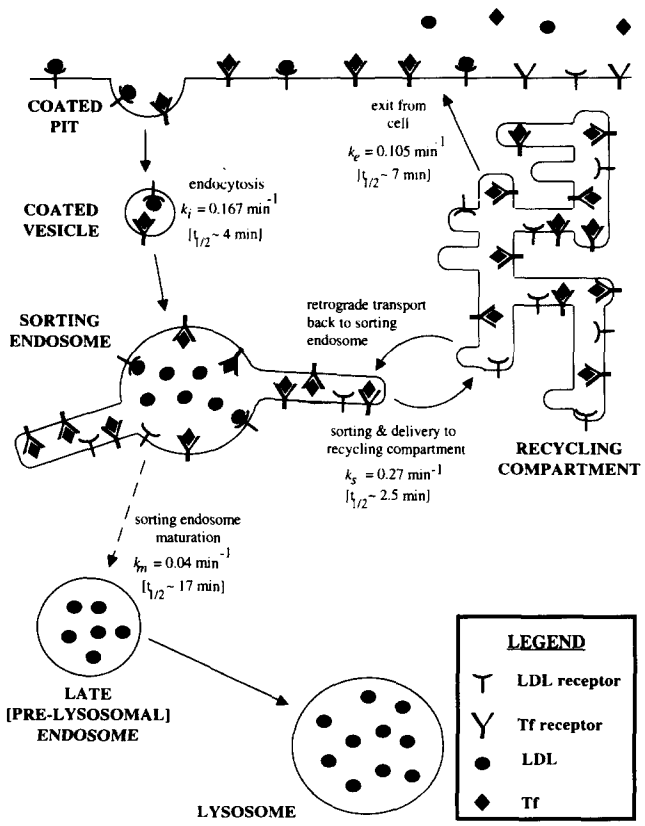

Figure 7. Schematic diagram of Tf and LDL trafficking in HEp2 cells. Tf and LDL are internalized by their respective receptors in coated pits. They are delivered to sorting endosomes via coated vesicles, where the LDL comes off its receptor and accumulates in the bulk volume. Tf, still bound to its receptor, and the LDL receptor are distributed along the membrane area of the sorting endosome and its tubular extensions. Tf and LDL sort with a half-time of ~2.5 min in the forward direction. Tf and the LDL receptor are then delivered to the recycling compartment. By a retrograde pathway, Tf is delivered back to the sorting endosome from the recycling compartment, where it comes to steady-state with the forward transported Tf. Tf leaves the cell with a 5.3–7.7-min half-time. LDL but not Tf, accumulates in the sorting endosome, which eventually loses its ability to receive newly endocytosed material and matures into a late endosome with approximately a 17-min half-time.

the result of (*a*) vesicles containing Tf budding from the recycling compartment and specifically targeted to the sorting endosome; or (*b*) error in the system resulting in misfusion of vesicles carrying Tf from the recycling compartment to the plasma membrane. The consequence of having Tf delivered back to sorting endosomes is that the sorting and recycling of Tf is less efficient than in a vectorial pathway. In the scheme of Dunn et al. (1989), where the iterative removal of membrane components is the basis for achieving high efficiency sorting, the presence of excess Tf in sorting endosomes from retrograde delivery implies that more iterations would be needed to achieve the same efficiency of sorting. Nevertheless, the same high sorting efficiency would be achieved in a slightly longer period of time, even with retrograde flow from the recycling compartment back to the sorting endosome.

Nonvectorial protein trafficking also occurs in the biosynthetic pathway in cells (Lippincott-Schwartz, 1993). In the vectorial route, proteins being synthesized are transported from the ER to the Golgi apparatus. However, a nonvectorial pathway from the Golgi back to the ER is used to retrieve resident ER proteins that have reached the Golgi. The nonvectorial pathway in the endocytic system may be playing a similar role as a mechanism for the maintenance of proper protein compositions among the different endosomal compartments. Hydrolytic lysosomal enzymes have been detected in endosomes of some cells at early times, suggesting that they are present in early sorting endosomes, and that their delivery to early endosomes is presumably from the Golgi apparatus (Diment and Stahl, 1985; Bowser and Murphy, 1990; Murphy, 1991). Thus, early endosomes may have input from multiple sources.

The recycling compartment is a long-lived organelle, as shown in studies on CHO cells. It is still accessible by endocytosed macromolecules along the recycling pathway after long periods of time (Salzman and Maxfield, 1989). It also has the ability to further sort and differentially retain molecules (Presley et al., 1993; Marsh, E. W., P. L. Leopold and F. R. Maxfield, unpublished results). Thus, this organelle may direct its constituents towards several destinations, and one of these is the retrograde trafficking to sorting endosomes. In addition, the recycling compartment's retentive ability may act to prevent the delivery of some proteins found in early endosomes to the plasma membrane.

Substantial experimental evidence in support of the maturation of early sorting endosomes has been obtained (Murphy, 1991; Stoorvogel et al., 1991; Dunn and Maxfield, 1992; van Deurs et al., 1993; Ghosh et al., 1994). A conceptual problem with a maturation mechanism is that it is not clear how sorting endosomes, which are transient organelles, would acquire the proteins needed for their specialized functions (Griffiths and Gruenberg, 1991). Based on our evidence for nonvectorial retrograde trafficking, the long-lived recycling compartment could act as a reservoir of proteins to be delivered back to the sorting endosome. The short-lived sorting endosomes could achieve a different protein composition than late endosomes if the appropriate proteins were delivered to sorting endosomes from the stable recycling compartment, and proteins specific to sorting endosomes but not late endosomes could be delivered back to the recycling compartment by the forward vectorial pathway.

The retrograde delivery of Tf back to sorting endosomes may not be a mechanism needed for proper cellular functioning, but instead, it could be the result of misdirection of vesicles from the recycling compartment. Sorting endosomes may have a lipid and protein composition similar to the plasma membrane, and they may contain the same factors used at the plasma membrane to mediate recycling vesicle fusion. Thus, retrograde flow to sorting endosomes could be the consequence of Tf-carrying vesicles that were supposed to fuse with the plasma membrane but, instead, fused with sorting endosomes. It is also possible that retrograde transport can occur along other parts of the endocytic pathway, and there exists evidence of fast exit of Tf from sorting endosomes, implying that a small amount of recycling occurs rapidly from sorting endosomes back to the plasma membrane without going through the recycling compartments (Presley et al., 1993).

We have shown that nonvectorial trafficking is occurring

in the endocytic system. Such bidirectional membrane traffic has been seen to occur in other trafficking systems in the cell, such as between the endoplasmic reticulum and the Golgi apparatus, where it is vital for the sorting and proper retention of resident ER proteins (Lippincott-Schwartz, 1993). The nonvectorial traffic in the endocytic system may be playing a similar role in maintaining the differences between the different endosomal compartments.

We would like to acknowledge the invaluable help of Dana Gelman, who did all the ^{125}I-Tf experiments and photography for this paper. We thank Michael Hillmeyer for sustained help in computer related matters, Jeffrey Myers and Xiaohui Zha for making and providing the fluorescent LDLs, and K. Sam Wells (Molecular Probes) for his gift of BODIPY-Tf. We also thank Kenneth Dunn, Satyajit Mayor, Timothy McGraw, and John Presley for critically reading the manuscript.

This work was supported by a fellowship from the New York City affiliate of the American Heart Association to R. N. Ghosh and a grant from the National Institutes of Health (DK27083) to F. R. Maxfield.

Received for publication 3 February 1994 and in revised form 10 November 1994.

References

Bowser, R., and R. F. Murphy. 1990. Kinetics of hydrolysis of endocytosed substrates by mammalian cultured cells: early introduction of lysosomal enzymes into the endocytic pathway. *J. Cell. Physiol.* 143:110–117.

Diment, S., and P. Stahl. 1985. Macrophage endosomes contain proteases which degrade endocytosed protein ligands. *J. Biol. Chem.* 260:15311–15317.

Dunn, K. W., and F. R. Maxfield. 1992. Delivery of ligands from sorting endosomes to late endosomes occurs by maturation of sorting endosomes. *J. Cell Biol.* 117:301–310.

Dunn, K. W., T. E. McGraw, and F. R. Maxfield. 1989. Iterative fractionation of recycling receptors from lysosomally destined ligands in an early sorting endosome. *J. Cell Biol.* 109:3303–3314.

Geuze, H. J., J. W. Slot, G. J. A. M. Strous, H. F. Lodish, and A. L. Schwartz. 1983. Intracellular site of asialoglycoprotein receptor-ligand uncoupling: double-label immunoelectron microscopy during receptor-mediated endocytosis. *Cell.* 32:277–287.

Ghosh, R. N., D. L. Gelman, and F. R. Maxfield. 1994. Quantification of low density lipoprotein and transferrin endocytic sorting in HEp2 cells using confocal microscopy. *J. Cell Sci.* 107:2177–2189.

Goldstein, J. L., S. K. Basu, and M. S. Brown. 1983. Receptor-mediated endocytosis of low-density lipoprotein in cultured cells. *Methods Enzymol.* 98:241–260.

Goud, B., and M. McCaffrey. 1991. Small GTP-binding proteins and their role in transport. *Curr. Opin. Cell Biol.* 3:626–633.

Griffiths, G., and J. Gruenberg. 1991. The arguments for pre-existing early and late endosomes. *Trends Cell Biol.* 1:5–9.

Hopkins, C. R., A. Gibson, M. Shipman, and K. Miller. 1990. Movement of internalized ligand-receptor complexes along a continuous endosomal reticulum. *Nature (Lond.).* 346:335–339.

Lippincott-Schwartz, J. 1993. Bidirectional membrane traffic between the endoplasmic reticulum and Golgi apparatus. *Trends Cell Biol.* 3:81–88.

Mattia, E., K. Rao, D. S. Shapiro, H. H. Sussman, and R. D. Klausner. 1984. Biosynthetic regulation of the human transferrin receptor by desferrioxamine in K562 cells. *J. Biol. Chem.* 259:2689–2692.

Maxfield, F. R., and K. Dunn. 1990. Studies of endocytosis using image intensification fluorescence microscopy and digital image analysis. *In* Optical Microscopy for Biology. B. Herman and K. Jacobson, editors. Wiley-Liss, Inc., New York. pp. 357–371.

Mayor, S., J. F. Presley, and F. R. Maxfield. 1993. Sorting of membrane components from endosomes and subsequent recycling to the cell surface occurs by a bulk flow process. *J. Cell Biol.* 121:1257–1269.

McGraw, T. E., and F. R. Maxfield. 1990. Human transferrin receptor internalization is partially dependent upon an aromatic amino acid on the cytoplasmic domain. *Cell Regul.* 1:369–377.

McGraw, T. E., and F. R. Maxfield. 1991. Internalization and sorting of macromolecules: endocytosis. *In* Targeted Drug Delivery. R. L. Juliano, editor. Springer-Verlag, Berlin. pp. 11–41.

McGraw, T. E., K. W. Dunn, and F. R. Maxfield. 1993. Isolation of a temperature-sensitive variant Chinese hamster ovary cell line with a morphologically altered endocytic recycling compartment. *J. Cell. Physiol.* 155: 579–594.

Murphy, R. F. 1991. Maturation models for endosome and lysosome biogenesis. *Trends Cell Biol.* 1:77–82.

Pagano, R. E., M. A. Sepanski, and O. C. Martin. 1989. Molecular trapping of a fluorescent ceramide analogue at the Golgi apparatus of fixed cells: interaction with endogenous lipids provides a *trans*-Golgi marker for both light and electron microscopy. *J. Cell Biol.* 109:2067–2079.

Pfeffer, S. R. 1992. GTP-binding proteins in intracellular transport. *Trends Cell Biol.* 2:41–45.

Pitas, R. E., T. L. Innerarity, J. N. Weinstein, and R. W. Mahley. 1981. Acetoacetylated lipoproteins used to distinguish fibroblasts from macrophages in vitro by fluorescence microscopy. *Arteriosclerosis.* 1:177–185.

Presley, J. F., S. Mayor, K. W. Dunn, L. S. Johnson, T. E. McGraw, and F. R. Maxfield. 1993. The End2 mutation in CHO cells slows the exit of transferrin receptors from the recycling compartment but bulk membrane recycling is unaffected. *J. Cell Biol.* 122:1231–1241.

Salzman, N. H., and F. R. Maxfield. 1988. Intracellular fusion of sequentially formed endocytic compartments. *J. Cell Biol.* 106:1083–1091.

Salzman, N. H., and F. R. Maxfield. 1989. Fusion accessibility of endocytic compartments along the recycling and lysosomal endocytic pathways in intact cells. *J. Cell Biol.* 109:2097–2104.

Schmid, S. L., R. Fuchs, P. Male, and I. Mellman. 1988. Two distinct subpopulations of endosomes involved in membrane recycling and transport to lysosomes. *Cell.* 52:73–83.

Snider, M. D., and O. C. Rogers. 1985. Intracellular movement of cell surface receptors after endocytosis: resialylation of asialo-transferrin receptor in human erythroleukemia cells. *J. Cell Biol.* 100:826–834.

Stoorvogel, W., H. J. Geuze, and G. J. Strous. 1987. Sorting of endocytosed transferrin and asialoglycoprotein occurs immediately after internalization in HepG2 cells. *J. Cell Biol.* 104:1261–1268.

Stoorvogel, W., H. J. Geuze, J. M. Griffith, and G. J. Strous. 1988. The pathways of endocytosed transferrin and secretory protein are connected in the *trans*-Golgi reticulum. *J. Cell Biol.* 106:1821–1829.

Stoorvogel, W., G. J. Strous, H. J. Geuze, V. Oorschot, and A. L. Schwartz. 1991. Late endosomes derive from early endosomes by maturation. *Cell.* 65:417–427.

Thomas, J., R. N. Buchsbaum, A. Zimniak, and E. Racker. 1979. Intracellular pH measurements in Ehrlich ascites tumor cells utilizing spectroscopic probes generated in situ. *Biochemistry.* 18:2210–2218.

Tooze, J., and M. Hollinshead. 1991. Tubular early endosomal networks in AtT20 and other cells. *J. Cell Biol.* 115:635–653.

van Deurs, B., P. K. Holm, L. Kayser, K. Sandvig, and S. H. Hansen. 1993. Multivesicular bodies in HEp-2 cells are maturing endosomes. *Eur. J. Cell Biol.* 61:208–224.

van Deurs, B., O. W. Petersen, S. Olsnes, and K. Sandvig. 1989. The ways of endocytosis. *Int. Rev. Cytol.* 117:131–177.

Wells, K. S., D. R. Sandison, J. Strickler, and W. W. Webb. 1990. Quantitative fluorescence imaging with laser scanning confocal microscopy. *In* Handbook of Biological Confocal Microscopy. J. B. Pawley, editor. Plenum Publishing Corp., New York. pp. 27–39.

Yamashiro, D. J., B. Tycko, S. R. Fluss, and F. R. Maxfield. 1984. Segregation of transferrin to a mildly acidic (pH 6.5) *para*-Golgi compartment in the recycling pathway. *Cell.* 37:789–800.